

# THE JLAB UV UNDULATOR

Stephen Gottschalk, STI Optronics, Bellevue, WA 98004, USA  
 Stephen Benson, Wesley Moore, JLAB, Newport News, VA, 23608, USA

## Abstract

Recently the JLAB FEL has demonstrated 150 W at 400 nm and 200 W at 700 nm\* using a 33-mm period undulator designed and built by STI Optronics. This paper describes the undulator design and performance. Two key requirements were low-phase error, zero steering, and offset end fields and small rms trajectory errors. We will describe a new genetic algorithm that allowed phase error minimization to 1.8 degrees while exceeding specifications. The mechanical design, control system and EPICS interface and lasing results will be summarized.

## INTRODUCTION

The UV undulator for JLAB has an interesting history. Originally in 2005 it used the magnetic subsystem consisting of magnets, poles, holders and beams for a 33-mm period undulator built by STI in 1988 for CHES. In 2011 those parts were returned to CHES and replaced by an APS "Undulator A" 33-mm period magnetic system originally built by STI in 1998 and used for LEUTL[1]. The LEUTL application was at a fixed gap of 9.35mm. It is the performance of the newer, variable gap system that is described in this paper.

## UNDULATOR DESIGN, PERFORMANCE, EPICS SUPPORT AND TUNING

A picture of the device installed at JLAB is shown in Fig. 1. The magnetic design of APS Undulator A 33-mm period has been described elsewhere [2]. Seven poles and magnets were removed from each end to accommodate the existing JLAB vacuum tube. All original shims and other tuning devices were removed by APS prior to shipment to STI. Without shims, phase error was below 5° but trajectory and quadrupoles needed tuning. The specification and performance are summarized in Table 1. A comparison of the original straight-pole CHES wiggler field strength with the present wedged pole APS wiggler is shown in Fig. 2. The wedged design is 25% stronger and the new wiggler has half the phase error.

The peak-to-peak trajectory error is important since it relates to keeping the electron beam in the middle of the optical mode. When the Rayleigh range is about one third of the wiggler length it is important to keep the electron beam centered on the optical mode to get the best

overlap. One can have a mode that has good gain with a plane wave but not with a tight Gaussian mode. In this case we have both. Angular errors can lead to phase errors but they can also compensate field errors to make the phase errors even smaller.



Figure 1: UV wiggler installed at JLAB.

The mechanical design was based on an earlier STI design for the JLAB IR wiggler [3]. Each beam is attached to two trolleys that move on linear guides. A total of four motors are used. A welded steel support frame is used for rigidity. Long bias coils provide ambient field compensation. The IR wiggler had a horizontal B field while the UV has a conventional vertical B-field. The UV wiggler added tilt switches and increased drive power since magnetic forces are larger. A Mitsubishi PLC was included in both systems, but it does not perform motion tasks. It is used as a watchdog to monitor mains, tilt switches, controlled stop, pause and emergency stop functions. The control panel is shown in Fig. 3.

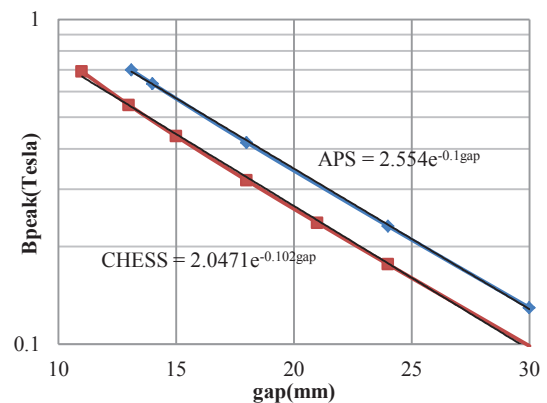


Figure 2: Field strengths of CHES and APS wigglers.

\* S. V. Benson et al., "Beam Line Commissioning of a UV/VUV FEL at Jefferson Lab", presented at the 2011 FEL Conference, Shanghai, China, Aug. 2011

Table 1: Summary of Wiggler Performance

Item	Specification	After tuning
Number of motors	4	4
Encoders	Load and motor	Load and motor
Period	33mm	33 mm
Gap range	11 – 100 mm	13.1 – 100.7
Magnetic CL shift	$\pm 100 \mu\text{m}$	$\pm 3 \mu\text{m}$
Gap resolution	$< 1 \mu\text{m}$	50 nm
Gap reproducibility	$< 20 \mu\text{m}$	$< 3 \mu\text{m}$
Cant angle variation	$< 1 \text{ mr}$	0.001 mr
Max end-to-end gap taper	$< 15 \mu\text{m}$	$5.3 \pm 13 \mu\text{m}$ at 13.1mm $8.0 \pm 29 \mu\text{m}$ at 29 mm
Pole-to-pole length	$< 213 \text{ cm}$	193
$ I1 $ , all gaps, both components	$< 400 \text{ G-cm}$	-4 to -56 G-cm normal -60 to -15 G-cm skew
$ I2 $ , all gaps	$< 20,000 \text{ G-cm}^2$ skew $< 10,000 \text{ G-cm}^2$ normal	-3900 to 2700 $\text{G-cm}^2$ normal -5300 to -200 $\text{G-cm}^2$ skew
Entrance offset	$< 10,000 \text{ G-cm}^2$	+710 $\text{G-cm}^2$ to -1060 $\text{G-cm}^2$
Quadrupole	$< 50 \text{ G}$ normal $< 50 \text{ G}$ skew	1.4 to 46.7 G normal 6.8 to -17.1 skew
Sextupole	$< 200 \text{ G/cm}$ normal $< 100 \text{ G/cm}$ skew	-73 to -25 G/cm normal 15 to 33 G/cm skew
Octupole	$< 300 \text{ G/cm}^2$ normal $< 50 \text{ G/cm}^2$ skew	$< 10 \text{ G/cm}^2$ both
Rolloff at 3mm	$< 0.1\%$	0.005%
Phase error	$< 5 \text{ degs}$	1.8 deg at 13.1 mm gap 1.03 deg at 29 mm gap
Peak field variation, 13.1 to 30mm gap	$< 1\%$	0.43% at 13.1 mm to 0.83% at 29mm gaps
Trajectory straightness at 150 MeV	$\pm 40 \mu\text{m} \sqrt{1 + (0.308 B_{rms} (kG))^2}$	-11 $\mu\text{m}$ to +8 $\mu\text{m}$ at 13.1mm -31 $\mu\text{m}$ to 17 $\mu\text{m}$ at 29mm



Figure 3: IR and UV wiggler control rack.

A Galil 4-axis motion controller provided closed-loop servo control using STI embedded firmware. Servo drives move Exlar linear actuators. The controller handles all synchronization, correction, safety, and status reporting. It moves all drives simultaneously. Ethernet is used for commands and status, RS232 is also available. Embedded firmware rejects unsafe movement requests such as taper or out-of-range gaps. During operation the controller accepts host ASCII commands, processes them and provides high-level status at 10 Hz. If needed, low-level UDP/IP packets can be queried up to 1 kHz. Linear

encoders or correction tables are used for accuracy. Encoder offsets are set so the system undershoots the gap and then moves slightly closer. For safety, there is no correction at minimum gap. Heidenhain metrology gages were used to measure half gap for each motor. Hard stops, limit switches as well as firmware, software, user gap limits, and zero-backlash fail-safe brakes provide additional levels of safety. During operation the drives can move to the requested gap, stop, engage the brakes, turn off and then no further motion occurs. Expert level GUI software was also written by STI. The operator GUI is an object-oriented programming, multi-tiered extension of the LNLS [4] and permanent magnet quadrupole [5] software. Galil firmware is quite similar between all these devices.

### *EPICS Support*

Since the embedded firmware manages all closed-loop control, process control was not a requirement for the EPICS support. However, it was essential in providing distributed access and control over both the IR[3] and UV wigglers. Using an EDM screen, the end user can request positioning based on K value or desired wavelength. This information along with the current energy of the electron beam is interpolated to determine the gap required to meet the request. The calculated gap is verified to be within a safe range before allowing the user to issue the change in wiggler gap. Changing the motor speed and monitoring the brake status are also provided to the user. Exposing the full functionality of the firmware could have been easily implemented, but was not a requirement at the time of commissioning. Only 18 process variables (PVs) were used for each wiggler, creating this basic set of controls and readbacks.

The Galil motion controller provides Ethernet and serial communication. Ethernet was used to create a local network between a PC hosting STI's expert control and the IR[3] and UV wigglers. At that time, the EPICS controls were hosted on a MVME177 IOC with available serial ports. Since then, COTS device servers along with the use of softIOCs have replaced the high-priced VME components. This maintains full flexibility for any future demands. For example, feedback provided by the EPICS controls is being merged with the JLAB FEL's laser safety system.

### *Genetic Shimming Algorithms*

As specifications have become more stringent, earlier tuning approaches have been upgraded to use global optimizers. For short wigglers, such as the Echo-7, NLCTA devices [9], true global optimization using linear/integer programming (LP) was feasible. Because the number of possible shim settings on long devices such as this one can be very large, heuristic, "good enough" approaches are used.

Rather than write a new simulated annealing code we used an Excel add-in Evolver from Pallisade. Population size was 50, crossover was 0.5, and mutation was 0.1.

Others [6-8] have used MatLAB or Igor for this purpose. The advantage of a genetic approach is that it does not require linear or quadratic equations and allows explicit minimization of phase errors. For the UV wiggler we used both pole shims [10] and magnet shims [2]. Since pole shims change the local gap, they are exactly equivalent to "virtual shimming". Different B-field signature functions were used for each type of shim. Additional features not used for [10] were modifying the thickness of existing shims; not allowing trajectory shims in regions with multipole shims and mixing pole and magnet shims. The processes of multipole, trajectory and end field tuning were interleaved.

To reach a small phase error we ran a number of scenarios to guide shim iterations (see Fig.4, upper right). For each scenario the number of shims was increased and the phase error had an upper constraint that was always smaller than the prior scenario. Agreement between predictions and measurements was remarkably good for each scenario. For 16 shims with a maximum thickness of 0.002", the phase error was 4.27 degrees but by allowing up to 64 pole shims with a few 0.006" thick shims the phase error of 1.8 degrees was reached. The thickness histogram is shown in Fig.4 upper left. During optimization at each scenario specification driven hard constraints on 1<sup>st</sup> and 2<sup>nd</sup> integrals, peak-to-peak trajectory, peak-to-peak angle, rms trajectory, B field and half-period kick were imposed.

We did note that about half the field errors did not have the same gap dependence as pole shims. This has been observed before and is why both pole and magnet shims are allowed. The tuning code is being upgraded to include multiple-gap shim signature functions. The trajectory calculated from the measured field is shown in the lower part of Fig. 4. Entrance angle and trajectory offset correlate (Fig. 4 lower, right) and are within specifications. No EM correctors were used to meet requirements.

## **LASING RESULTS**

The UV laser was commissioned with the new undulator and lased with three different mirror sets. The first, centered at 700 nm lased well. During commissioning, lasing was achieved on a satellite peak of the mirror wavelength detuning curve where the losses were over 50% per pass. The second set was the 400 nm set used in previous measurements. The detector system used to measure the gain was not functioning correctly. The measured gain was higher than 100% but the turn-on and cavity length detuning curves were consistent with the values recorded with the previous wiggler, which demonstrated electronic gain of approximately 180% per pass. Finally we lased with a hole coupler at 373 nm and delivered 10 eV third harmonic light to experiments studying atomic trapping of krypton. Tuning across each of the mirror sets was easily achieved.

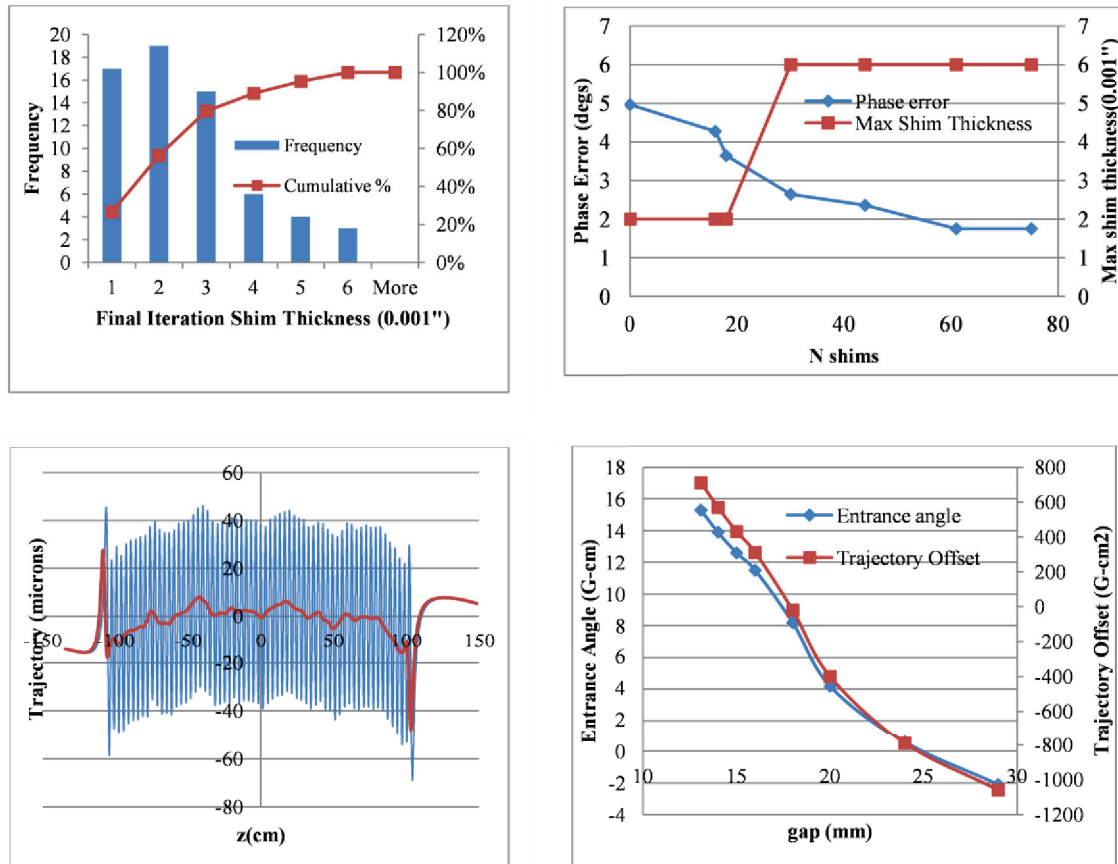


Figure 4: Final UV wiggler trajectory at 13.1-mm gap (lower, left), entrance condition (lower, right), shim details (upper).

## CONCLUSION

We have described the design and performance of the JLAB UV wiggler and described steps used for tuning with a genetic optimizer.

## REFERENCES

- [1] S.V. Milton, "Measurements of Exponential Gain and Saturation at the APS LEUTL", PAC 2001, p. 236-240 (2001).
- [2] K. Robinson, et al, "Advances in Undulator Technology at STI Optronics", Rev. Sci. Instr. 67 (9), September 1996, paper C06.
- [3] G. R. Neil et al., "The JLab High Power ERL Light Source", Nucl. Instr. & Meth. **A557** p. 9 (2006).
- [4] R.H.A. Farias, et al, "Commissioning of the LNLS 2T Hybrid Wiggler", PAC2005, p. 1072-1074 (2005).
- [5] S. Gottschalk, et al, "Performance of an Adjustable Strength Permanent Magnet Quadrupole", PAC2005, p. 2071-2073 (2005).
- [6] O. Chubar, et al, "Application of Genetic Algorithms to Sorting, Swapping and Shimming of SOLEIL Undulator Magnets", SRT-2006, AIP Conf. Proc. Vol.879, p.359 (2006).
- [7] M. Rynnänen, "Characterisation and optimisation of hybrid insertion devices using genetic algorithms", University of Helsinki 2004, University of Helsinki, Report Series in Physics, HU-P-D122, p. 93 (2004).
- [8] O. Rudenko, et al, "An Evolutionary Approach to Shimming Undulator Magnets for Synchrotron Radiation Sources", Proc. 9th Int. Conf. on Parallel Problem Solving from Nature PPSN IX, p. 362 (2006).
- [9] S. Gottschalk "Design and Performance of the NLCTA-Echo 7 Undulators", this conference.
- [10] S. Gottschalk et al., "Design and Performance of the Wedged Pole Hybrid Undulator for the Fritz-Haber-Institut IR FEL", this conference.